BIOCHEMISTRY
including biophysical chemistry & molecular biology

Article

pubs.acs.org/biochemistry

Proline Kink Angle Distributions for GWALP23 in Lipid Bilayers of Different Thicknesses

Johanna M. Rankenberg,[†] Vitaly V. Vostrikov,[†] Christopher D. DuVall,[†] Denise V. Greathouse,[†] Roger E. Koeppe, II,*[,†] Christopher V. Grant,[‡] and Stanley J. Opella[‡]

[†]Department of Chemistry and Biochemistry, University of Arkansas, Fayetteville, Arkansas 72701, United States

[‡]Department of Chemistry and Biochemistry, University of California, San Diego, La Jolla, California 92093, United States

Supporting Information

ABSTRACT: By using selected ^{2}H and ^{15}N labels, we have examined the influence of a central proline residue on the properties of a defined peptide that spans lipid bilayer membranes by solid-state nuclear magnetic resonance (NMR) spectroscopy. For this purpose, GWALP23 (acetyl-GGALW^{5}LALALALALALW^{19}LAGA-ethanolamide) is a suitable model peptide that employs, for the purpose of interfacial anchoring, only one tryptophan residue on either end of a central α-helical core sequence. Because of its systematic behavior in lipid bilayer membranes of differing thicknesses [Vostrikov, V. V., et al. (2010) *J. Biol. Chem. 285*, 31723−31730], we utilize GWALP23 as a well-characterized framework for introducing guest residues within a transmembrane sequence; for example, a central proline yields acetyl-GGALW^{5}LALALAP^{12}ALALALW^{19}LAGA-ethanolamide. We synthesized GWALP23-P12 with specifically placed ^{2}H and ^{15}N labels for solid-state NMR spectroscopy and examined the peptide orientation and segmental tilt in oriented DMPC lipid bilayer membranes using combined ^{2}H GALA and $^{15}N-^{1}H$ high-resolution separated local field methods. In DMPC bilayer membranes, the peptide segments N-terminal and C-terminal to the proline are both tilted substantially with respect to the bilayer normal, by ∼34 ± 5° and 29 ± 5°, respectively. While the tilt increases for both segments when proline is present, the range and extent of the individual segment motions are comparable to or smaller than those of the entire GWALP23 peptide in bilayer membranes. In DMPC, the proline induces a kink of ∼30 ± 5°, with an apparent helix unwinding or "swivel" angle of ∼70°. In DLPC and DOPC, on the basis of ^{2}H NMR data only, the kink angle and swivel angle probability distributions overlap those of DMPC, yet the most probable kink angle appears to be somewhat smaller than in DMPC. As has been described for GWALP23 itself, the C-terminal helix ends before Ala^{21} in the phospholipids DMPC and DLPC yet remains intact through Ala^{21} in DOPC. The dynamics of bilayer-incorporated, membrane-spanning GWALP23 and GWALP23-P12 are less extensive than those observed for WALP family peptides that have more than two interfacial Trp residues.

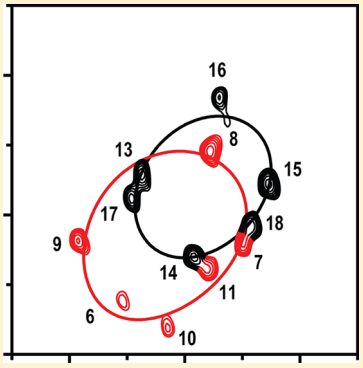

The functions of membrane proteins are sometimes reliant on the presence and positioning of specific proline residues,[1−5] which may introduce a kink within a transmembrane helical sequence. To examine the consequences of proline on structure and dynamics, it is of interest to study the effects of a proline residue within model transmembrane peptide sequences. Significant unresolved questions pertain not only to an overall kink angle but also to the peptide dynamics and the orientations of individual segments on either side of the proline with respect to a lipid bilayer normal. Some of these issues have been addressed using a system in which two Trp anchors flank a central transmembrane helical core sequence, WALP19, acetyl-GWW(LA)$_6$LWWA-ethanolamide.[6] Nevertheless, some of the system properties are difficult to interpret when too many interfacial tryptophans are present. Multiple Trp anchors tend to complicate the behavior of transmembrane peptides, for example, by inducing significant peptide dynamics and variations in the helix tilt direction.[7] Remarkably, the extent of dynamic averaging of NMR resonances is reduced when only two Trp residues, or one Trp and one Tyr, are present.[8] Therefore, with only single Trp anchors near each membrane interface, the transmembrane peptide behavior has been found to be more predictable and systematic with respect to the helix tilt magnitude, direction, and lipid bilayer thickness.[7−10]

Here we characterize a central proline residue within the context of a transmembrane peptide having only one Trp anchor near each end, using lipid bilayers of varying thickness. For this purpose, we incorporated proline into GWALP23,[9] resulting in GWALP23-P12 (acetyl-GGALWLALALA-P^{12}ALALALWLAGA-ethanolamide). GWALP23 itself (Figure 1) exhibits a well-defined, tilted transmembrane orientation that scales with lipid bilayer thickness.[7,8] To study the effects of proline incorporation on the behavior of GWALP23, we incorporated ^{2}H-labeled Ala or ^{15}N-labeled Leu and Ala residues at specific positions within the sequence, on both sides of the proline.

Received: February 29, 2012
Revised: April 10, 2012
Published: April 10, 2012

   dx.doi.org/10.1021/bi300281k | *Biochemistry* 2012, 51, 3554−3564

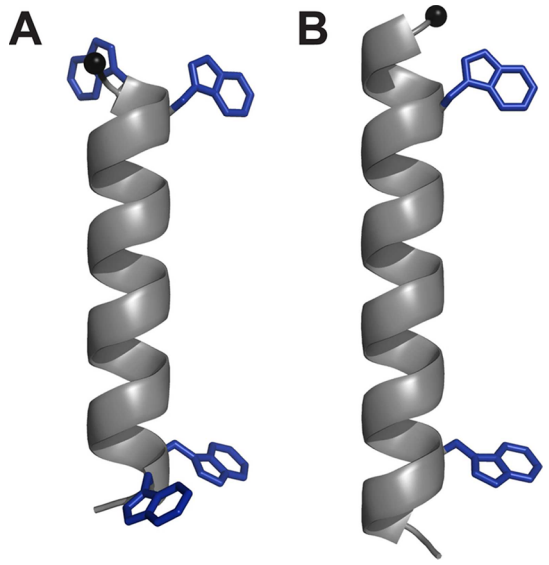

Figure 1. Representative models of (A) WALP19 with four Trp residues and (B) GWALP23 with only two Trp residues. The core helical sequence between the inner tryptophans is identical in the two peptides. The Trp indole side chains are shown in arbitrary orientations (see also Table 1).

When considering the helix breaking properties of proline, the N-terminal domain is both expected and observed to be more sensitive,[6] because a hydrogen bond is missing between the proline residue and the amino acid four residues earlier in the sequence. The distortion introduced into the transmembrane helix by the proline, which effectively divides the continuous α-helix into two sections, is of interest for characterization, in terms of not only the helix kink angle but also the individual tilt magnitudes and directions for the N- and C-terminal domains. If sufficient data can be obtained, aspects of the segmental dynamics also can be characterized. For this reason, deuterium quadrupolar splitting values from ^{2}H-labeled Ala residues[11] are used together with ^{15}N−^{1}H dipolar coupling and ^{15}N chemical shift values from ^{15}N-labeled Ala and ^{15}N-labeled Leu residues,[9,12,13] allowing a combined ^{2}H and ^{15}N solid-state NMR analysis of the properties of the GWALP23-P12 helical segments in DMPC.

The combined use of the ^{15}N- and ^{2}H-based solid-state NMR techniques, analyzed together, provides a robust determination of the peptide properties. Advantages are offered by both the complementary nature of these NMR techniques and the significant number of data points available for each peptide segment. Considering that GWALP23 has a relatively long α-helical domain with only one anchoring Trp residue near each end, this peptide is a favorable candidate for such studies. The insertion of Pro at position 12 in the transmembrane core of GWALP23 is expected to preserve sufficiently long α-helical segments for the determination of the orientations of the segments on both sides of the proline.

Previous work from our lab revealed that the proline residue in WALP19-P10 interrupts the helix and results in two segments with distinct orientations and a kink angle of ∼20° in DOPC bilayers.[6] Uncertainties remain, nevertheless, concerning the respective N- and C-terminal segment orientations and dynamics. The presence of only single Trp anchors and the availability of ^{15}N data have allowed us to obtain additional information about GWALP23-P12.

MATERIALS AND METHODS

Fmoc-amino acids and resin were obtained from Novabiochem (San Diego, CA) or Advanced Chemtech (Louisville, KY). Isotope-enriched [^{15}N]Fmoc-L-amino acids were from Cambridge Isotope Laboratiories (Andover, MA) and Sigma-Aldrich (St. Louis, MO). Deuterium-labeled alanine and ^{2}H-depleted water were from Cambridge. This commercial L-alanine-d_4 was Fmoc-protected using Fmoc-ON-succinimide (Novabiochem), as described previously.[14] Ethanolamine and trifluoroethanol (TFE) were from Sigma-Aldrich. All lipids (DH-o-PC, DLPC, DMPC, DM-o-PC, and DOPC) were acquired from Avanti polar lipids (Alabaster, AL). Other solvents were the highest grade available from EMD (Gibbstown, NJ).

Peptide synthesis was performed on an Applied Biosystems 433A peptide synthesizer (Life Technologies, Foster City, CA), using modified Fmoc chemistry with extended coupling times and additional deprotection steps. L-Ala-d_4 or ^{15}N-labeled amino acids were incorporated at specific residues during peptide synthesis. Using a dual labeling strategy, deuterated alanine was incorporated at 100% abundance and at lower 50% abundance in two different sequence positions, in the same peptide.[15] During peptide synthesis, a 5-fold excess of Fmoc-amino acid was used for unlabeled residues and for [^{15}N]Leu and [^{15}N]Ala. A 2-fold excess of Fmoc-L-Ala-d_4 followed by a second coupling with a 5-fold excess of unlabeled Fmoc-L-Ala was used for deuterated alanines.[16] Protecting groups, *N*-acetyl and *C*-ethanolamide, served to mask the charges at the ends of the peptides. The *C*-ethanolamide group was introduced during cleavage of a peptide from Wang resin, using 20% ethanolamine in dichloromethane, for 48 h under constant agitation at 22 °C.[17] The reaction was quenched using deionized water, upon which the peptide precipitated. The precipitated peptide was centrifuged to form a pellet, which was lyophilized twice from 1 mL of an acetonitrile/water mixture (1:1, v/v). The purity of peptides was evaluated via reversed-phase HPLC using a 4.6 mm × 50 mm Zorbax SB-C8 column packed with 3.5 μm octylsilica (Agilent Technologies, Santa Clara, CA), operated at 1 mL/min using a methanol/water gradient from 85 to 99% methanol over 5 min. The peptide identity was confirmed using MALDI mass spectrometry.

Samples for NMR spectroscopy were prepared using peptides listed in Table 1. Mechanically oriented samples for deuterium NMR spectroscopy were prepared with a 1:40 peptide:lipid ratio using DLPC, DMPC, or DOPC. Magnetically oriented samples for high-resolution separated local field (SLF) experiments (SAMPI4)[18] were prepared using a 1:80 peptide:long-chain lipid ratio, DMPC for deuterium studies or DM-o-PC for ^{15}N-based studies, in addition to short-chain lipid DH-o-PC present to allow bicelle formation. The ether-linked lipids DM-o-PC and DH-o-PC, chosen for some experiments on the basis of their superior chemical stability, exhibit behavior similar to that of the corresponding ester lipids DMPC and dihexanoyl-PC.[19,20]

For the preparation of mechanically oriented samples, a peptide/lipid mixture was made from 2 μmol of peptide in a TFE stock solution and 80 μmol of lipid in chloroform. Solvents were evaporated under a stream of N_2, followed by drying under vacuum (10^{-3} Torr) for at least 24 h. The peptide/lipid mixture was dissolved in 95% methanol and 5% water and distributed evenly over ∼40 glass slides [4.8 mm × 23 mm × 0.07 mm (Marienfeld, Lauda-Königshofen, Germany)]. The slides with the mixture were placed under

dx.doi.org/10.1021/bi300281k | *Biochemistry* 2012, 51, 3554−3564

vacuum for at least 48 h, after which the peptide/lipid films were hydrated using deuterium-depleted water to a hydration level of 45% (w/w). The hydrated slides were stacked under gentle pressure and then sealed in a glass cuvette. To allow for formation and alignment of lipid bilayers, we incubated the samples for at least 48 h at 42 °C. To verify the orientation of mechanically aligned bilayers, we recorded solid-state ^{31}P NMR spectra (^{1}H-decoupled) at 50 °C using a Bruker Avance 300 spectrometer (Bruker Instruments, Billerica, MA).

Bicelle samples, which contain lipid bilayer disks that orient in a magnetic field, were made using 0.76 μmol of ^{2}H- or ^{15}N-labeled peptide, 61 μmol of DM-o-PC (or DMPC), and 19 μmol of DH-o-PC, giving a value of 3.2 for the q ratio of long to short lipid. The peptide in TFE and DM-o-PC in chloroform were mixed together in appropriate amounts. Solvents were evaporated under a flow of N_2 gas, and samples subsequently were dried under vacuum (10^{-3} Torr) for at least 36 h. The DMPC/peptide films were hydrated using 125 μL of deuterium-depleted water at 45 °C, resulting in the formation of multilamellar vesicles, which were further mixed with DH-o-PC suspended in 50 μL of deuterium-depleted water. To promote bicelle formation, a series of freeze−thaw steps were performed until a clear solution with a low viscosity at a low temperature (~4 °C) was obtained. (An increase in temperature results in an increased sample viscosity up to the point of ~45 °C, upon which the viscosity decreases again.) Samples were transferred to 5 mm glass vials (New Era Enterprises, Vineland, NJ) and sealed in preparation for NMR experiments.

Deuterium NMR spectra were recorded at 46 MHz using a Bruker Avance 300 spectrometer, employing a quadrupolar echo sequence with full phase cycling,[21] a 4.5 μs 90° pulse time, a 90 ms recycle delay, and a 125 μs echo delay. The sample temperature was 50 °C for glass slides and 42 °C for bicelles. The ^{2}H spectra were processed using 200 Hz line broadening. Deuterium quadrupolar splitting values were assigned to individual labeled alanine methyl groups on the basis of the distances between corresponding peak maxima and the relative peak intensities associated with the respective isotopic abundances used for particular residues in the peptide sequence.

For ^{15}N-enriched peptides, ^{15}N chemical shifts and ^{15}N−^{1}H dipolar coupling values were recorded using 500 MHz Bruker Avance and Varian Inova spectrometers and established pulse sequences.[13,18,22−24] Solid-state NMR high-resolution separated local field SAMPI4 experiments (which are complementary to PISEMA)[18] were performed using a 1 ms CP contact time, RF field strengths of approximately 50 kHz; 54 t_1 points were acquired using an acquisition time of 8.0 ms in the direct (t_2) dimension and a 7.5 s recycle delay. The sample temperature was 42 °C.

Combinations of ^{2}H quadrupolar splitting magnitudes, along with ^{15}N chemical shift and ^{15}N−^{1}H dipolar coupling values, were used to calculate the orientations of the different peptide segments in DMPC. We performed these calculations both with a semistatic model and with a more dynamic model that incorporates Gaussian distributions for the tilt and direction of tilt.[25]

The analysis using semistatic peptide dynamics involves a principal order parameter S_{zz} to estimate the overall peptide motion with respect to an apparent average peptide orientation. These calculations are based on the GALA analysis, eqs 1 and 3, as previously described.[11,25,26] We incorporate also ^{15}N−^{1}H dipolar coupling and ^{15}N chemical shift values obtained from SAMPI4 spectra, using eqs 2, 4 and 5, to determine the best fit to the experimental data.[27] These calculations are performed using τ, ρ and S_{zz} as variable parameters to fit the data for the isotope-labeled residues based on ideal α-helix geometry.

$$\Delta\nu_{\mathrm{q}} = \mathrm{QCC} \times S_{zz}\left[\frac{1}{2}(3\cos^2\theta - 1)\right]\left[\frac{1}{2}(3\cos^2\beta - 1)\right] \quad (1)$$

$$\Delta\nu_{\mathrm{HN}} = \mathrm{DCC} \times S_{zz}\left[\frac{1}{2}(3\cos^2\theta - 1)\right]\left[\frac{1}{2}(3\cos^2\beta - 1)\right] \quad (2)$$

$$\mathrm{QCC} = \frac{3}{2}\frac{e^2qQ}{h} \quad (3)$$

$$\mathrm{DCC} = \frac{\mu_0\gamma_{\mathrm{N}}\gamma_{\mathrm{H}}\hbar}{4\pi r_{\mathrm{N-H}}^{3}} \quad (4)$$

The general equation for the chemical shift is:

$$\sigma_{\mathrm{static}} = \sigma_{11}H_{11}^{2} + \sigma_{22}H_{22}^{2} + \sigma_{33}H_{33}^{2} \quad (5)$$

In eq 5, the σ_{ii} values are the chemical shift tensor components and H_{ii} values the corresponding projections of the applied magnetic field. The chemical shift tensor components σ_{11}, σ_{22}, and σ_{33} were 64, 77, and 224 ppm, respectively, as reported previously for model dipeptides[28] and small proteins.[29] Chemical shift values were converted from parts per million to hertz, and a principal order parameter S_{zz} was applied as described previously.[30] The dependence of the ^{15}N chemical shift on θ has been described previously.[12,13,30]

The quadrupolar splitting, eq 1, depends upon the static coupling constant QCC, which is defined in eq 3 and has a value that is $^{1}/_{3}$ of 168 kHz, namely 56 kHz, for CD_3 groups.[6,11] Other parameters include the orientation angle θ for the alanine C_α−C_β bond with respect to the bilayer normal and the macroscopic sample orientation angle β for the bilayer normal with respect to the external magnetic field. The peptide geometry is reflected in angle $\varepsilon_\parallel$ between the peptide helix axis and the C_α−C_β bond vector for deuterium-labeled alanine residues.[11] θ depends on the peptide geometry ($\varepsilon_\parallel$) and the orientation of the peptide's helix axis (τ and ρ). While earlier analysis[11] involved searching for appropriate values of $\varepsilon_\parallel$, the current procedure fixes $\varepsilon_\parallel$ at a known appropriate value of 59.4° and varies S_{zz} to estimate the dynamics and obtain a best fit.

The dipolar coupling values are dependent on a coupling constant of 10.22 kHz (assuming a N−H bond length of 1.06 Å in eq 4),[31,32] and the angle θ that in turn is dependent on τ, ρ, and $\varepsilon_\parallel$. For an α-helical peptide, defined by angles Φ, Ψ, and Ω of −65°, −40°, and 180°,[33] respectively, $\varepsilon_\parallel$ is 14° between the peptide helix axis and the N−H bond vector for ^{15}N-labeled residues. In the combined analysis, the ^{2}H methyl quadrupolar couplings, ^{15}N−^{1}H dipolar couplings, and ^{15}N chemical shifts were given equal weights; to account for peak dispersion and a poor signal-to-noise ratio, a relative weighting factor of 0.5 was applied to the observed and calculated backbone C_α−^{2}H quadrupolar couplings.

Using these equations and parameters, probable peptide segment orientations were calculated by considering the best fit [lowest root-mean-square deviation (rmsd) between calculated values and NMR observables] for a range of peptide orientations. Helix rotation ρ is referenced in relation to the C_α atom of the first amino acid (Gly^{1}) of the peptide.[11] To calculate a kink angle (κ) between two α-helical segments, one

considers both the tilt (τ) and rotation (ρ) differences between the segments N- and C-terminal to the proline (eq 6).[15]

$$\cos(\kappa) = \sin(\tau_N)\sin(\tau_C)\cos(\Delta\rho) + \cos(\tau_N)\cos(\tau_C) \quad (6)$$

We have also performed calculations that consider more complex peptide dynamics, in which $\sigma\tau$ and $\sigma\rho$ describe the widths of Gaussian distributions for the peptide tilt and rotation, respectively.[25] In this analysis, a principal order parameter S_{zz} is set to 0.88 to estimate isotropic fluctuations,[25] and further anisotropic variations in τ and ρ are then described by fitting $\sigma\tau$ and $\sigma\rho$.[25] A best-fit rmsd to observed dipolar and quadrupolar couplings is based on the parameters τ, ρ, $\sigma\tau$, and $\sigma\rho$, following ref 25. Whereas the semistatic analysis employs three parameters, the Gaussian analysis involves a four-parameter fit.

RESULTS

The synthetic GWALP23-P12 peptides gave the predicted molecular mass and isotope enrichment values (Figure S1 of the Supporting Information) and were at least 95% pure as determined by reversed-phase HPLC (Figure S2 of the Supporting Information).

Peptides were incorporated into mechanically or magnetically aligned lipid bilayers. Oriented glass-plate samples were prepared using peptides containing specific deuterated alanine residues. To confirm the mechanical alignment of the bilayers, ^{31}P NMR spectra were recorded (Figure S3 of the Supporting Information). From the ^{2}H NMR spectra for samples aligned with a β of 90° (Figures 2 and 3) or with a β of 0° (Figures S4 and S5 of the Supporting Information), unique quadrupolar splitting magnitudes were observed for each labeled alanine in the sequence. Resonances were assigned to the corresponding alanine residues on the basis of relative signal intensities, bearing in mind the isotopic abundance present for each of the

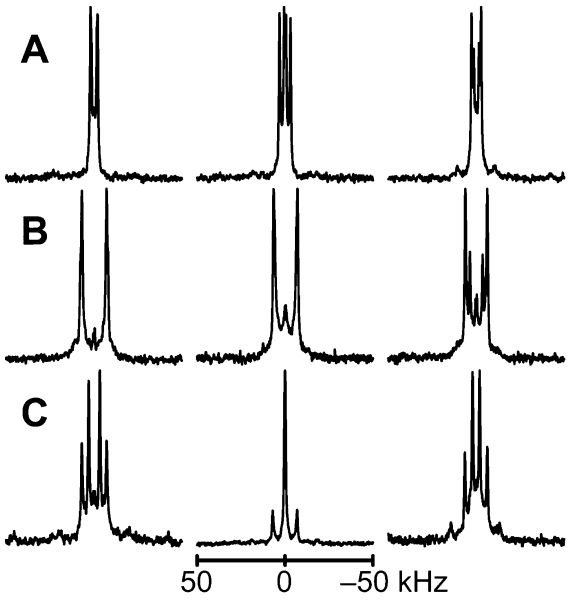

Figure 2. ^{2}H NMR spectra for labeled Ala methyl groups C-terminal to the proline in GWALP23-P12, in oriented bilayers of DLPC, DMPC, and DOPC. The sample orientation is β = 90°. Deuterium isotope levels in the labeled alanines are (A) 100% Ala^{17} and 50% Ala^{21}, (B) 100% Ala^{15} and 50% Ala^{13}, and (C) 100% Ala^{16} and 50% Ala^{15}.

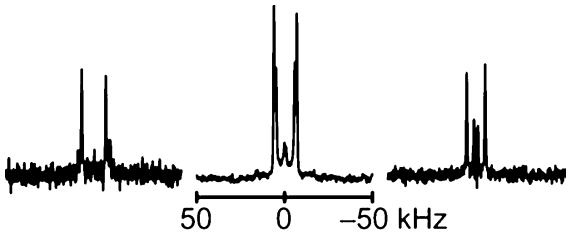

Figure 3. ^{2}H NMR spectra for labeled Ala methyl groups N-terminal to the proline in GWALP23-P12, in oriented bilayers of DLPC, DMPC, and DOPC (from left to right, respectively). The sample orientation is β = 90°. The deuterium isotope abundance is 100% in Ala^{7} and 50% in Ala^{9}.

labeled residues (Table 1). The observed quadrupolar splitting magnitudes (reported in Table 2 for the β = 0° orientation) were reduced by a factor of 2, as expected, when a sample was turned from β = 0° to β = 90°.

Bicelle samples for magnetic alignment were prepared using ^{15}N-labeled Leu and Ala at positions 13−17 (five residues) C-terminal to the proline or positions 5−11 and 13−18 (six residues on either side of the proline). The SAMPI4 spectrum for residues 13−17 was compared to that for the same residues in GWALP23. These spectra, each showing only five signals, can be assigned in unique fashion (Figure 4) for a right-handed α-helix, because the signals from residues 13 and 17 must be near each other on a helical wheel and the helix sense is known. The spectral overlay (Figure 4) also reveals a larger spread of the five assigned peaks when proline 12 is present. For example, the ^{1}H−^{15}N dipolar couplings for residues 13−17 range from 1.3 to 3.5 kHz when P12 is present (Table 3) but only from 2.4 to 3.8 kHz for GWALP23 without the proline.[30] The shift of the centroid of the pattern of five peaks (Figure 4) suggests a somewhat different tilt for the C-terminal helical segment of GWALP23 when P12 is present. The expanded size ("diameter") of the pattern may indicate somewhat reduced motional averaging of the NMR observables when P12 is present. Further analysis of the segmental orientation and dynamics follows.

The full SAMPI4 spectrum (Figure 5) shows a striking pattern that indicates directly the presence of two helical wheels with different tilt angles in the DMPC/DHPC bicelles. With the peaks for residues 13−17 assigned, the remaining peaks for residue 18 and residues 6−11 were assigned by considering a difference spectrum, the right-handed α-helix geometry, the absence of a signal for proline 12, and a distortion from helical geometry at residue 11, adjacent to the proline (Figure 5). The assigned resonances on the PISA wheels yield directions of tilt (see below), for the segments C- and N-terminal to proline, that are consistent with the tilt directions deduced independently from GALA analysis of deuterated alanines alone. Dipolar coupling and ^{15}N chemical shift values were recorded (Table 3) for the labeled residues on the basis of the assigned PISA wheel peaks. (As noted in Table 3, the values for residue 11 were excluded from the analysis because the helix is broken at that location. Helix distortion also has been observed for the residue preceding Pro in WALP19-P10.[6])

When not only ^{2}H quadrupolar coupling magnitudes but also ^{15}N chemical shifts and ^{15}N−^{1}H dipolar coupling values are available, namely for the case of DMPC bilayers (in combination with DM-o-PC/DH-o-PC bicelle samples), the segment orientations can be determined using a combined

dx.doi.org/10.1021/bi300281k | Biochemistry 2012, 51, 3554−3564

Table 1. Sequences of Peptides[a]

WALP19-P10	acetyl-GWWLALALA**P**ALALALWWA-ethanolamide
GWALP23-P12	acetyl-GGALWLALALA**P**ALALALWLAGA-ethanolamide
A[16]GWALP23-P12	acetyl-GGALWLALALA**P**ALA**A**ALWLAGA-ethanolamide

[a]WALP19-P10 is included for reference. Labels were incorporated for ^{2}H and ^{15}N NMR experiments. Deuterium labels were introduced in two alanines per GWALP23-P12 peptide, using partial (p) and full (f) deuteration at the following positions: 7[f] and 9[p], 13[p] and 15[f], 17[f] and 21[p], and 15[p] and 16[f] (in the mutant A[16]GWALP23-P12 sequence). Two GWALP23-P12 peptides were synthesized with uniform ^{15}N enrichment, covering residues 13−17 or residues 6−11 together with residues 13−18.

Table 2. Observed ^{2}H Quadrupolar Splitting Magnitudes for Labeled Alanines in GWALP23-P12[a]

Ala	DLPC	DMPC	DOPC
7	27.6	26.8	21.2
9	36.9	20.8	4.4
13	28.5	25.4	14.3
15	28.5	27.6	25.0
15[b]	28.0	28.0	25.9
16	12.3	0.5[c]	8.1
17	8.2	12.2	6.0
21	7.2[c]	2.2[c]	10.2
9[d]		66[d]	
21[d]	89[d]	70[d]	53[d]

[a]Values in kilohertz for the β = 0° sample orientation. Values represent the CD_3 side chain except where noted. [b]Values for A15 when A16 replaces L16. [c]Value not used for tilt analysis. [d]Backbone C_α deuteron.

Table 3. Dipolar Couplings and ^{15}N Chemical Shifts for ^{15}N−^{1}H Groups in GWALP23-P12[a]

residue	^{15}N−^{1}H dipolar coupling (kHz)	^{15}N chemical shift (ppm)
6	0.7	111.0
7	1.5	89.8
8	2.8	95.6
9	1.5	118.5
10	0.3	103.0
11[b]	1.2[b]	96.2[b]
13	2.4	107.5
14	1.3	98.5
15	2.3	85.5
16	3.5	94.0
17	2.1	109.3
18	1.7	88.5

[a]Values are listed for bicelle samples, corresponding to a β = 90° sample orientation. [b]Values for residue 11 were excluded from the analysis of the N-terminal segment because the helix is broken at this point.

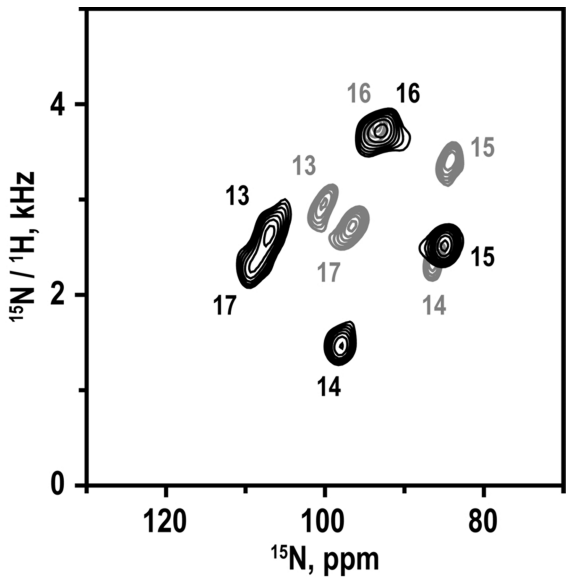

Figure 4. Overlay of SAMPI4 spectra for ^{15}N-labeled residues 13−17 in GWALP23 (gray) and GWALP23-P12 (black), with the peak assignments indicated.

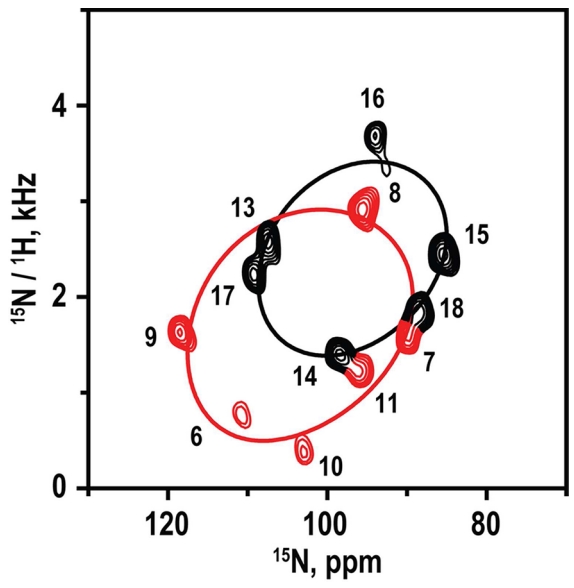

Figure 5. SAMPI4 spectrum for ^{15}N-labeled residues 6−11 and 13−18 of GWALP23-P12 in magnetically oriented DM-o-PC/DH-o-PC bicelle bilayers. The spectrum was recorded from a single sample. Peaks were assigned by comparison with the spectrum for residues 13−17 (Figure 4) and are colored red for residues N-terminal to the proline. Helical ("PISA") wheel patterns are superimposed to represent the orientations of the N-terminal and C-terminal segments (Table 4).

analysis involving all available data (Table 4). For the respective temperatures of ∼50 °C for bilayers and ∼42 °C for bicelles, it has been determined that the peptide principal order parameter is similar between the two systems.[30] The analysis is based on calculation models in which the theoretical quadrupolar and dipolar waves, together with the distribution of ^{15}N chemical shifts, most closely approximate the values found experimen-

Table 4. Calculated Orientations in DMPC of Segments N- and C-Terminal to Proline in GWALP23-P12, Using Gaussian Dynamics and Semistatic Calculation Models[a]

segment	model	τ_0	σ_τ	ρ_0	σ_ρ	S_{zz}	rmsd	n^b
N-terminal	Gaussian	35°	18°	263°	36°	0.88[c]	1.1 kHz	13 (2 + 1 + 5 + 5)
	semistatic	30°	na[d]	263°	na[d]	0.64	1.1 kHz	13 (2 + 1 + 5 + 5)
C-terminal	Gaussian	29°	0°	329°	48°	0.88[c]	0.9 kHz	15 (3 + 0 + 6 + 6)
	semistatic	22°	na[d]	332°	na[d]	0.72	1.0 kHz	15 (3 + 0 + 6 + 6)

[a]The Gaussian model for the dynamics uses a fixed principal order parameter S_{zz},[25] representing the dynamic extent of (mis)alignment (angle α) between the molecular z-axis and its average orientation, characterized by the time average $S_{zz} = \langle 3\cos^2\alpha - 1\rangle/2$.[34] Within this context, further motions can be characterized by widths σ_τ and σ_ρ of Gaussian distributions about the average values of tilt magnitude τ_0 and tilt direction ρ_0.[25] An alternative semistatic analysis, using three parameters instead of four, determines the best fit (lowest rmsd) as a function of τ_0, ρ_0, and S_{zz}. Weighting factors for the ^{2}H methyl and backbone quadrupolar couplings, ^{1}H−^{15}N dipolar couplings, and ^{15}N chemical shifts were 1.0, 0.5, 1.0, and 1.0, respectively. [b]Total number of data points in the format (^{2}H methyl, ^{2}H backbone, ^{1}H−^{15}N dipolar, and ^{15}N chemical shift). [c]Fixed value. [d]Not applicable.

tally, as determined by an rmsd. We determined average apparent peptide segment orientations in DMPC using both semistatic and Gaussian dynamic approximations (see Table 4). The results indicate a tilt of the N-terminal segment of ∼30° for a semistatic model or a closely similar value of 34° for a Gaussian analysis, with a corresponding $\sigma\tau$ of 19°. The tilt angle observed for the C-terminal segment is 22° for a semistatic model or ∼29° with a $\sigma\tau$ of notably 0° for a converged Gaussian dynamic analysis. The direction of tilt ρ_0 for the N-terminal segment is ∼263° for either dynamic model (relative to the Gly[1] C_α atom), while the semistatic and Gaussian analyses also agree with the direction of C-terminal segment tilt and yield a value of ∼330° (Table 4). The GWALP23 helix itself exhibits a ρ_0 of ∼312° (when proline is absent), so the respective segmental tilt changes in direction are approximately −50° and 20°, giving a proline-induced difference in the direction of segment tilt ($|\Delta\rho_0|$) of ∼70°. The Gaussian analysis indicates substantial $\sigma\rho$ values of ∼34° for the N-terminal segment and ∼48° for the C-terminal segment. We note that the larger $\sigma\rho$ value for the C-terminus together with the larger $\sigma\tau$ value for the N-terminus may suggest the presence of some coupled dynamics (see Discussion). The distributions of results are evident in the calculated dipolar wave plots (Figure 6) and in rmsd plots for τ_0 and ρ_0 and for $\sigma\tau$ and $\sigma\rho$ (Figures 7 and 8). Once again, the observed segmental tilt parameters should be compared to the reported τ_0 and ρ_0 values of 9° and 312°, respectively, for GWALP23 in DMPC, in the absence of the proline.[7] The central proline increases the magnitude of tilt for both segments, with respect to the DMPC bilayer normal, while exerting opposite effects on the N- and C-terminal segment tilt directions.

Using the orientations determined for the segments on each side of the proline residue, it is feasible to calculate a kink (κ) angle introduced into the peptide as described in eq 6. From the segment orientations shown in Figure 8, we calculated a probability distribution for the κ value for GWALP23-P12 in DMPC. The most probable κ value is ∼30 ± 5° (Figure 9B). As noted, the helix unwinding or "swivel" angle ($|\Delta\rho_0|$) is 65−70° in DMPC, regardless of the method employed for the dynamic analysis.

The segment analysis in lipids other than DMPC is less straightforward because ^{15}N data are not available. To increase somewhat the size of the ^{2}H data sets for the C-terminus in DLPC and DOPC, we included a variation in which a substitution (L16A) could provide an additional data point. This type of substitution often has only a small effect on the helical properties of the peptide segment C-terminal to Pro and

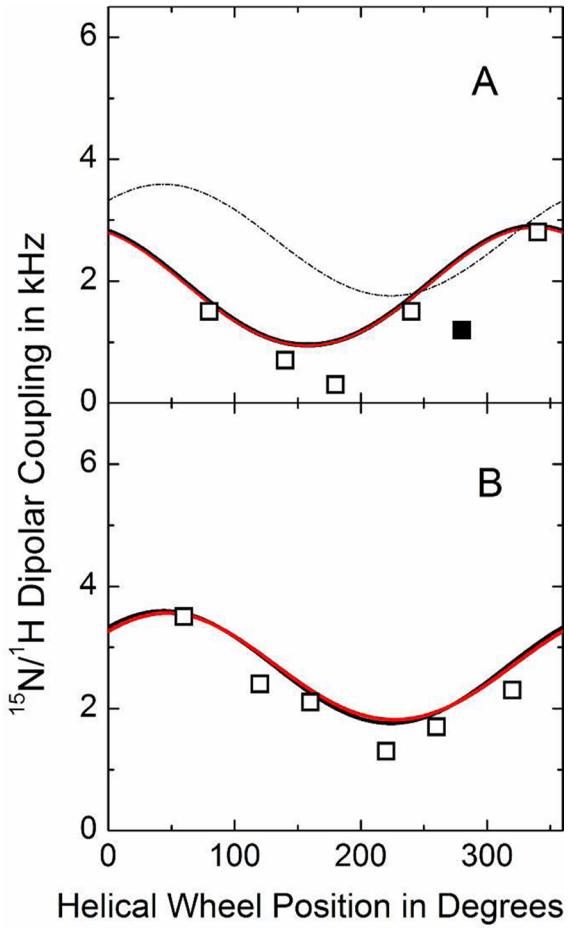

Figure 6. Calculated dipolar wave plots for the N-terminal (A) and C-terminal (B) segments of GWALP23-P12 in oriented DMPC bilayers. Wave functions based on semistatic (red) or Gaussian (black) calculations essentially overlap. Data points indicated by empty symbols have been used in the calculations, whereas the filled symbol represents a measurement for A11 that was excluded from the analysis (because the helix is broken prior to P12). For comparison, the fit to the C-terminus (B) is included also in the form of the thin dashed curve in panel A.

therefore is likely to fit the GALA wave and provide valuable additional quadrupolar splitting values.[6] As described above, we incorporated a control label (Ala[15]) adjacent to the L16A substitution. The ^{2}H NMR spectra indicate that the control residue 15 changed little (Table 2) when the L16A substitution was introduced. Because the segment N-terminal to proline can

dx.doi.org/10.1021/bi300281k | Biochemistry 2012, 51, 3554−3564

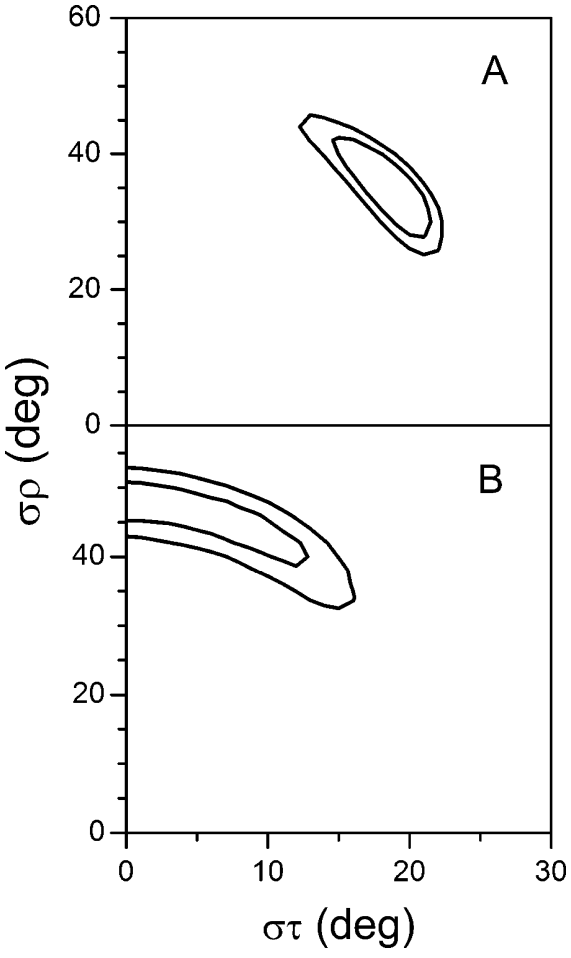

Figure 7. Gaussian dynamics. rmsd ($\sigma\tau$ and $\sigma\rho$) graphs for the Gaussian dynamics analysis of the N-terminal (A) and C-terminal (B) helical segments of GWALP23-P12 in oriented DMPC bilayers. Contours are drawn at 1.3 and 1.5 kHz (A) or 0.9 and 1.0 kHz (B).

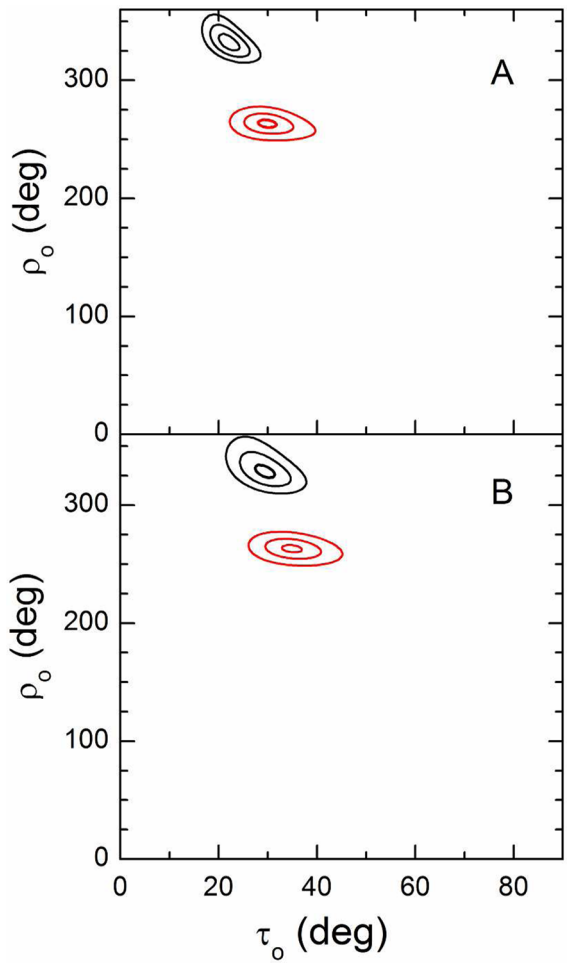

Figure 8. Segmental tilt. rmsd plots for the tilt of the N-terminal (red) and C-terminal (black) helical segments of GWALP23-P12 in oriented DMPC bilayers. (A) rmsd plotted as a function of τ and ρ for the optimal S_{zz} in semistatic calculations. (B) rmsd plotted as a function of τ and ρ for the optimal values of $\sigma\tau$ and $\sigma\rho$ in Gaussian calculations (see Figure 7 and Table 4). The rmsd contour levels are 1, 2, and 3 kHz.

be more sensitive to mutations,[6] mutations were not introduced into this region. Additional data points for both segments emerged fortuitously when the quadrupolar splittings were observed from the backbone C_α deuterons of residues 9 and 21 (Table 2). In lipids where the C-terminal segment remained helical through residue 21 (see below), both the backbone and side-chain ^{2}H signals for Ala^{21} could be employed in the analysis.

With the smaller numbers of data points, a Gaussian dynamic analysis of segmental tilt in DLPC or DOPC is not feasible at this time, as it leads to a high degeneracy of solutions. Nevertheless, we have estimated the allowed distributions of apparent tilt magnitudes τ_0 and directions ρ_0 for the segments in DLPC and DOPC (Figure S6 of the Supporting Information), based upon available ^{2}H quadrupolar splitting magnitudes and using (assumed) order parameters that are close to those deduced in DMPC. The semistatic estimates suggest modest segment adjustments in DLPC or DOPC. For the C-terminal segment, ρ_0 remains close to 330° in all three lipids, while τ_0 in DLPC or DOPC may decrease slightly (Figure S6 of the Supporting Information) from the value of 22° observed by semistatic analysis in DMPC (Figure 8A). For the N-terminal segment, with the caveat of limited data, the currently allowed ranges of τ_0 and ρ_0 are larger in DLPC and DOPC (Figure S6 of the Supporting Information). [For the kink analysis in DOPC, we considered only values within the major distribution of τ_0 between 0° and 45° and ρ_0 between 180° and 360° (Figure S6 of the Supporting Information).] When the segmental data are considered together, the resulting probability plots (Figure 9) suggest that the kink angle (κ) distributions for DLPC and DOPC overlap that for DMPC, although the most probable κ may be somewhat smaller in DLPC or DOPC than in DMPC. Figure S7 (see the Supporting Information) illustrates the swivel angle distributions for GWALP23-P12 in the three lipids. As is the case for DMPC, also in DLPC and DOPC the most probable swivel angle magnitude is ~70° ($\Delta\rho$ is −70° when expressed as $\rho_N - \rho_C$), although several other choices exhibit non-zero probability under the current data limitations (Figure S7 of the Supporting Information).

We also tested whether the C-terminal segment remains helical through a deuterated Ala^{21} residue. In parallel studies, it had been determined that the GWALP23 helix ends at or near Trp^{19}, namely in the region between residues 19 and 21.[7] We find a similar result for the C-terminal segment of GWALP23-P12 in DLPC and DMPC, although the segment nevertheless does remain helical for residues 13−21 in the thicker DOPC

dx.doi.org/10.1021/bi300281k | *Biochemistry* 2012, 51, 3554−3564

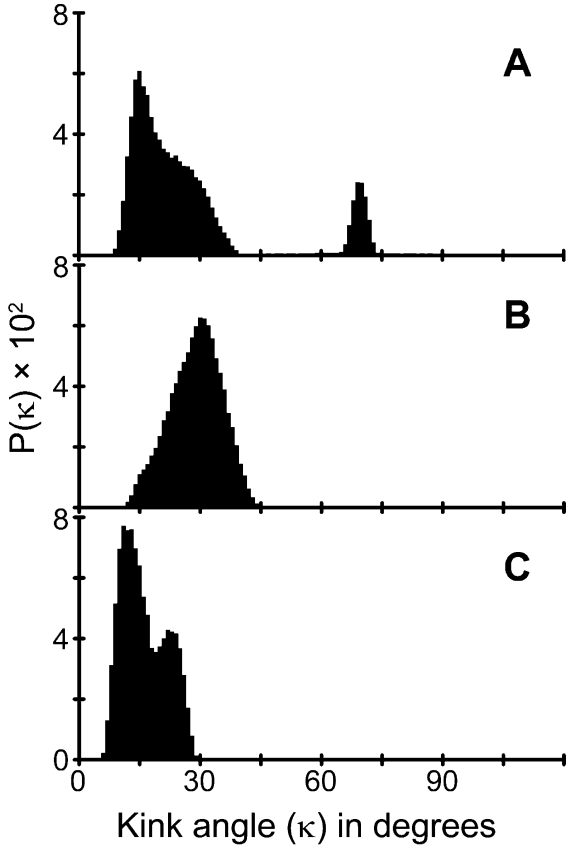

Figure 9. Distributions of apparent kink angles, κ (degrees), calculated from rmsd (τ and ρ) analysis of the N- and C-terminal segments of GWALP23-P12 in (A) DLPC, (B) DMPC, and (C) DOPC. Regions with an rmsd of <3 kHz (C-terminal) or <2 kHz (N-terminal) were binned at a τ of 1° and a ρ of 1°.

bilayer membranes. As a consequence, the quadrupolar splitting obtained for Ala[21] also could be used for the GALA analysis in DOPC but not in DLPC or DMPC. In Figure 10, we show the fitted semistatic GALA waves for the C-terminal segment in each of the lipid membranes. While the A21 data point (filled symbol) fits on a GALA curve for DOPC, the deviations of A21 from the best-fit quadrupolar waves exceed 5 kHz in both DLPC and DMPC. The lipid bilayer thickness influences the helicity of the C-terminal segment.

DISCUSSION

The biological occurrence of transmembrane proline-containing peptides is sufficiently common that it is important to understand the implications of the presence of a proline residue for the structure, dynamics, and positioning of a transmembrane sequence. The combined analysis of deuterium (^{2}H) and ^{15}N NMR spectral data, reported here, allowed a robust determination of a proline-induced kink angle in a designed model peptide in DMPC. We find that introduction of proline into a previously "ideal" GWALP23 α-helix introduces a moderately large kink angle that changes relatively little with lipid bilayer thickness. In the DLPC, DMPC, and DOPC lipids tested, the peptide segments on either side of the proline both adopt significant tilt angles with respect to the lipid membrane normal. Indeed, both segments increase their tilt angles, in comparison with the previously reported whole-peptide tilt of GWALP23 in each of the lipid bilayer membranes.[7]

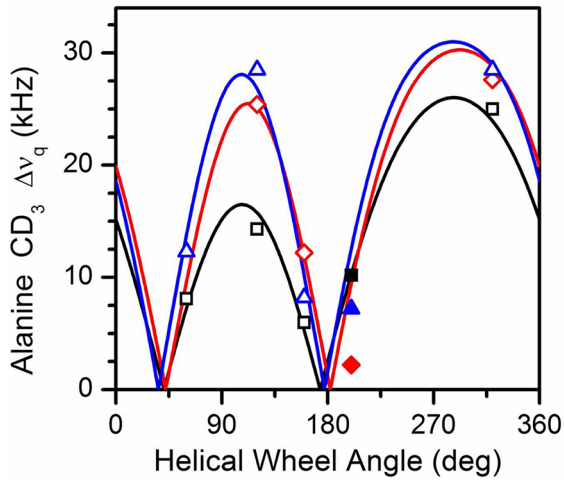

Figure 10. Quadrupolar waves from semistatic GALA analysis of the C-terminal segment of GWALP23-P12 in lipid bilayer membranes of DOPC (black), DMPC (red), and DLPC (blue). The solid symbols indicate data points for A21, which resides outside of the core region defined by W5 and W19. A21 remains part of the core helix in DOPC, but helix distortion moves the A21 quadrupolar splitting more than 5 kHz below the best-fit curves for DLPC and DMPC.

Remarkably, regardless of the host lipid identity, the segmental directions of tilt for the C-terminus of GWALP23-P12 remain the same in DLPC, DMPC, and DOPC (Figure 8 and Figure S6 of the Supporting Information). Compared to the reference GWALP23, the introduction of Pro[12] alters the C-terminal tilt direction by ~20°. In DMPC, the N-terminal tilt direction changes oppositely by ~50°, leading to a swivel or approximate helix unwinding angle of close to −70° (=$\rho_N - \rho_C$). With a caveat due to the data limitations, it appears likely that the swivel angle of approximately −70° is preserved in DLPC and DOPC (Figure S7 of the Supporting Information).

The use of combined ^{1}H−^{15}N high-resolution SLF and ^{2}H GALA-based solid-state NMR methodologies is advantageous for calculating the average apparent orientations of the segments before and after proline in GWALP23-P12 in lipid bilayers (bicelles) of DMPC (DM-o-PC). At the respective experimental temperatures, the peptide (segment) principal order parameters are approximately the same in the bilayers at 50 °C and in the bicelles at 42 °C. The combined data sets allow us to deduce a kink angle of ~30° in DMPC. We note that both segments increase their tilt, from ~9° for GWALP23 itself, with respect to the DMPC bilayer normal, when P12 is introduced (see Table 4).

The quality of the combined analysis, using data from macroscopically oriented DMPC bilayers (on glass slides) together with data from magnetically oriented DM-o-PC bicelles, suggests that not only segment motions but also the tilt parameters vary only slightly between the bilayer and bicelle samples. Furthermore, when the bicelle-derived ^{1}H−^{15}N SAMPI4 data (Figure 4 and Table 3) are analyzed alone, in the absence of the bilayer-derived ^{2}H quadrupolar splittings, the resulting apparent τ_0 value of 29° for the C-terminal segment is identical to that deduced from the combined bilayer and bicelle data (Table 4). The deduced ρ_0 values also are nearly identical from bicelles to bilayers, giving in each case a value of ~330 ± 2° for the C-terminal segment. Similarly, for the N-terminal segment, the deduced τ_0 remains nearly constant at 35−36° (Table 4), regardless of whether only the ^{15}N data or the full

dx.doi.org/10.1021/bi300281k | Biochemistry 2012, 51, 3554−3564

data sets are analyzed, while in this case, the apparent ρ_0 increases slightly, from 263° (for the full data sets) to 273° (^{15}N data only, in bicelles). To summarize, the SAMPI4 results from bicelle samples and the GALA results from bilayer samples agree closely for the tilt magnitude and direction for both of the helical segments, preceding and following the proline, in DMPC.

In addition to the calculation of the peptide tilt and rotation, simple visual observation of helical wheel representations with respect to the obtained SAMPI4 spectra provides a striking confirmation of the kink introduced by the proline. This can be recognized easily, as there are two distinct sets of resonances that fit to separate helical wheel patterns in the two-dimensional SAMPI4 spectrum (Figure 5).

The semistatic and Gaussian treatments of the dynamics of GWALP23-P12 in DMPC agree quite well. Considering the semistatic model, the peptide orientation consists of a 30°-tilted N-terminal segment connected to a 22°-tilted C-terminal segment via a 30° kink angle. The kink angle between the segments also reflects the −69° difference in rotation for the two segments, 263° and 332°, respectively. Considering the dynamic Gaussian model, we calculate a 35°-tilted N-terminus connected to the 29°-tilted C-terminus, with a −66° swivel angle (difference in rotation) and a 34° kink angle. Overall, the agreement is quite good between the two models for the analysis, as they give similar kink angles and nearly identical swivel angles. The magnitude of the 30−34° kink angle is somewhat larger than the value of 19° determined previously for WALP19 in DOPC.[6] The modest difference in the kink angle could reflect the different lipid environment and/or the different numbers of Trp anchor residues, as well as their positions relative to the proline ring. While "inner" Trp^3 and Trp^{17} of WALP19 have the same radial and longitudinal separation as Trp^5 and Trp^{19} of GWALP23, the "outer" Trp residues of WALP19 are absent in GWALP23.

The respective $\sigma\tau$ and $\sigma\rho$ values from the Gaussian analyses (Table 4) suggest slightly more rotational averaging for the C-terminal segment, together with a larger value of $\sigma\tau$ for the N-terminal segment. We note that the connecting proline should couple some of the segment motions, such that the C-terminal and N-terminal dynamics should not be completely independent. In this vein, rotation of the C-terminal helix could lead to tilt variation ($\sigma\tau$ motion) of the N-terminal helix, and vice versa. The extent of the helix wobble, nevertheless, can be larger than the change in an apparent τ value, because not all projections of wobbling motions will influence the angle between a helix axis and the membrane normal. The semistatic analysis by itself suggests furthermore a somewhat lower principal order parameter of 0.64 for the N-terminal segment (Table 4). The relative N-terminal mobility is in accord with the location of the missing hydrogen bond, before proline, and with previous observations that the segment preceding proline is more susceptible to helix unwinding.[3,6] Internal helix motions also would likely not be coupled through the proline.

The proline connection furthermore might decrease each segment's preferred range and extent of motion. Indeed, the larger sizes of the PISA wheels for both of the individual segments (Figures 4 and 5), compared to the PISA wheel of GWALP23 itself (Figure 4), suggest smaller extents of dynamic averaging for both the C-terminus and N-terminus when proline 12 is present in GWALP23.

In comparison to previous studies on the proline-containing WALP19-P10 in DOPC bilayers, we find for GWALP23-P12 in DMPC a modestly larger κ angle, 30−34° versus 19°, along with significantly larger τ angles for each of the proline-flanking segments, namely 30−35° and 22−29° versus 7° and 12°, respectively.[6] The greater hydrophobic length of GWALP23-P12 in the thinner DMPC bilayer probably accounts for the larger segmental tilt values, compared to those of WALP19-P10 in DOPC, while the influence on the proline-induced kink angle κ is somewhat less dramatic.

In addition to the studies of GWALP23-P12 in DMPC bilayers, we have performed ^{2}H NMR experiments using thicker and thinner lipid bilayer systems. Although fewer data points are available than in DMPC, we nevertheless estimate the allowed ranges of segmental tilt (Figure S6 of the Supporting Information) and the kink and swivel probabilities (Figure 9 and Figure S7 of the Supporting Information) in DLPC and DOPC. The results suggest modest yet non-systematic changes in the kink angle with bilayer thickness, as the most probable κ value, based on available data, may be slightly smaller in DLPC and DOPC than in DMPC. Because the C-terminal helix is intact through A21 in DOPC, but not in DMPC or DLPC, partial unwinding may represent a portion of the helix adaptation to the lipids. The entire segment preceding proline is furthermore susceptible to helix unwinding,[3,6] presumably to varying extents depending upon the immediate environment.

With regard to biological relevance, it is of note that an array of biologically occurring proline-containing transmembrane helices displays a wide range of proline-induced kink angles from 0° to 70°.[3] These results demonstrate the use of ^{1}H−^{15}N SAMPI4 and ^{2}H GALA solid-state NMR methods to determine the relative orientations of transmembrane helical segments on either side of a localized distortion. The methods should prove relevant for investigating α-helical transmembrane sequences containing a helix-breaking residue such as proline or glycine, also known for its potential helix breaking properties. In this context, one notes the advantages conferred by the joint application of ^{2}H and ^{15}N−^{1}H NMR methods, and furthermore the combined use of aligned lipid bicelle and lipid bilayer samples.

In summary, the full SAMPI4 spectrum (Figure 5) illustrates directly the kink in GWALP23-P12. The combined analysis of deuterium (^{2}H) and ^{1}H−^{15}N NMR observables has allowed the robust determination of the proline-induced kink angle in the designed peptide GWALP23-P12 in DMPC. For proteins, the influence of proline on domain orientation and dynamics could have decisive consequences, especially considering that structure and function are tightly intertwined. As a result, it is well acknowledged that cellular functions could be influenced critically by the presence or absence of specific transmembrane proline residues.

■ ASSOCIATED CONTENT

Supporting Information

Mass spectra, HPLC chromatogram, ^{31}P NMR spectra, and additional ^{2}H NMR spectra, to confirm peptide identity and purity, and the alignment of lipids and peptides. This material is available free of charge via the Internet at http://pubs.acs.org.

■ AUTHOR INFORMATION

Corresponding Author

*Address: 119 Chemistry Building, University of Arkansas, Fayetteville, AR 72701. Telephone: (479) 575-4976. Fax: (479) 575-4049. E-mail: rk2@uark.edu.

Funding

This work was supported in part by National Science Foundation Grant MCB 0841227 and by the Arkansas Biosciences Institute. The peptide facility was supported by National Institutes of Health (NIH) Grants RR31154 and RR16460. The ^{2}H NMR facility in Fayetteville, AR, was supported by NIH Grants RR31154 and GM103450. The ^{15}N NMR facility in La Jolla, CA, was supported by the Biotechnology Research Center for NMR Molecular Imaging of Proteins at the University of California, San Diego, which is supported by NIH Grant P41EB002031.

Notes

The authors declare no competing financial interest.

■ ACKNOWLEDGMENTS

We thank James Hinton and Marvin Leister for many helpful discussions.

■ ABBREVIATIONS

DH-o-PC, ether analogue of 1,2-dihexanoylphosphatidylcholine; DLPC, 1,2-dilauroylphosphatidylcholine; DMPC, 1,2-dimyristoylphosphatidylcholine; DM-o-PC, ether analogue of 1,2-dimyristoylphosphatidylcholine; DOPC, 1,2-dioleoylphosphatidylcholine; Fmoc, fluorenylmethoxycarbonyl; GALA, Geometric Analysis of Labeled Alanines; HPLC, high-performance liquid chromatography; MALDI, matrix-assisted laser desorption ionization; NMR, nuclear magnetic resonance; PISEMA, Polarization Inversion with Spin Exchange at Magic Angle; TEA, triethylamine; TFE, trifluoroethanol; TM, transmembrane; GWALP23, acetyl-GGALWLALALALALALALWLA-GA-ethanolamide.

■ REFERENCES

(1) Von Heijne, G. (1991) Proline kinks in transmembrane α-helices. *J. Mol. Biol. 218*, 499−503.

(2) Ulmschneider, M. B., and Sansom, M. S. (2001) Amino acid distributions in integral membrane protein structures. *Biochim. Biophys. Acta 1512*, 1−14.

(3) Cordes, F. S., Bright, J. N., and Sansom, M. S. P. (2002) Proline-Induced Distortions of Transmembrane Helices. *J. Mol. Biol. 323*, 951−960.

(4) Glukhov, E., Shulga, Y. V., Epand, R. F., Dicu, A. O., Topham, M. K., Deber, C. M., and Epand, R. M. (2007) Membrane interactions of the hydrophobic segment of diacylglycerol kinase epsilon. *Biochim. Biophys. Acta 1768*, 2549−2558.

(5) Decaffmeyer, M., Shulga, Y. V., Dicu, A. O., Thomas, A., Truant, R., Topham, M. K., Brasseur, R., and Epand, R. M. (2008) Determination of the topology of the hydrophobic segment of mammalian diacylglycerol kinase ϵ in a cell membrane and its relationship to predictions from modeling. *J. Mol. Biol. 383*, 797−809.

(6) Thomas, R., Vostrikov, V. V., Greathouse, D. V., and Koeppe, R. E., II (2009) Influence of proline upon the folding and geometry of the WALP19 transmembrane peptide. *Biochemistry 48*, 11883−11891.

(7) Vostrikov, V. V., Daily, A. E., Greathouse, D. V., and Koeppe, R. E., II (2010) Charged or aromatic anchor residue dependence of transmembrane peptide tilt. *J. Biol. Chem. 285*, 31723−31730.

(8) Gleason, N. J., Vostrikov, V. V., Greathouse, D. V., Grant, C. V., Opella, S. J., and Koeppe, R. E., II (2012) Tyrosine replacing tryptophan as an anchor in GWALP peptides. *Biochemistry 51*, 2044−2053.

(9) Vostrikov, V. V., Grant, C. V., Daily, A. E., Opella, S. J., and Koeppe, R. E., II (2008) Comparison of "Polarization inversion with spin exchange at magic angle" and "geometric analysis of labeled alanines" methods for transmembrane helix alignment. *J. Am. Chem. Soc. 130*, 12584−12585.

(10) Vostrikov, V. V., Hall, B. A., Greathouse, D. V., Koeppe, R. E., II, and Sansom, M. S. (2010) Changes in transmembrane helix alignment by arginine residues revealed by solid-state NMR experiments and coarse-grained MD simulations. *J. Am. Chem. Soc. 132*, 5803−5811.

(11) van der Wel, P. C. A., Strandberg, E., Killian, J. A., and Koeppe, R. E., II (2002) Geometry and intrinsic tilt of a tryptophan-anchored transmembrane α-helix determined by ^{2}H NMR. *Biophys. J. 83*, 1479−1488.

(12) Wang, J., Denny, J., Tian, C., Kim, S., Mo, Y., Kovacs, F., Song, Z., Nishimura, K., Gan, Z., Fu, R., Quine, J. R., and Cross, T. A. (2000) Imaging membrane protein helical wheels. *J. Magn. Reson. 144*, 162−167.

(13) Marassi, F. M., and Opella, S. J. (2000) A solid-state NMR index of helical membrane protein structure and topology. *J. Magn. Reson. 144*, 150−155.

(14) ten Kortenaar, P. B. W., Dijk, B. G., Peeters, J. M., Raagen, B. J., Adams, P. J., and Tesser, G. I. (1986) Rapid and efficient method for the preparation of Fmoc-amino acids starting from 9-fluorenylmethanol. *Int. J. Pept. Protein Res. 27*, 398−400.

(15) Daily, A. E., Greathouse, D. V., van der Wel, P. C. A., and Koeppe, R. E., II (2008) Helical distortion in tryptophan and lysine anchored membrane-spanning α helices as a function of hydrophobic mismatch: A solid-state deuterium NMR investigation using the GALA method. *Biophys. J. 94*, 480−491.

(16) Greathouse, D. V., Koeppe, R. E., II, Providence, L. L., Shobana, S., and Andersen, O. S. (1999) Design and characterization of gramicidin channels. *Methods Enzymol. 294*, 525−550.

(17) Greathouse, D. V., Goforth, Robyn, L., Crawford, T., van der Wel, P., and Killian, J. A. (2001) Optimized aminolysis conditions for cleavage of N-protected peptides from solid-phase resins. *J. Pept. Res. 57*, 519−527.

(18) Nevzorov, A. A., and Opella, S. J. (2007) Selective averaging for high-resolution solid-state NMR spectroscopy of aligned samples. *J. Magn. Reson. 185*, 59−70.

(19) Cavagnero, S., Dyson, H. J., and Wright, P. E. (1999) Improved low pH bicelle system for orienting macromolecules over a wide temperature range. *J. Biomol. NMR 13*, 387−391.

(20) Aussenac, F., Lavigne, B., and Dufourc, E. J. (2005) Toward bicelle stability with ether-linked phospholipids: Temperature, composition, and hydration diagrams by H-2 and P-31 solid-state NMR. *Langmuir 21*, 7129−7135.

(21) Davis, J. H., Jeffrey, K. R., Valic, M. I., Bloom, M., and Higgs, T. P. (1976) Quadrupolar echo deuteron magnetic resonance spectroscopy in ordered hydrocarbon chains. *Chem. Phys. Lett. 42*, 390−394.

(22) Wu, C. H., Ramamoorthy, A., and Opella, S. J. (1994) High-resolution heteronuclear dipolar solid-state NMR spectroscopy. *J. Magn. Reson., Ser. A 109*, 270−272.

(23) Nevzorov, A. A., and Opella, S. J. (2003) A "Magic Sandwich" pulse sequence with reduced offset dependence for high-resolution separated local field spectroscopy. *J. Magn. Reson. 164*, 182−186.

(24) Cook, G. A., and Opella, S. J. (2010) NMR studies of p7 protein from hepatitis C virus. *Eur. Biophys. J. Biophys. Lett. 39*, 1097−1104.

(25) Strandberg, E., Esteban-Martin, S., Saldago, J., and Ulrich, A. S. (2009) Orientation and dynamics of peptides in membranes calculated from ^{2}H-NMR data. *Biophys. J. 96*, 3223−3232.

(26) Strandberg, E., Özdirekcan, S., Rijkers, D. T. S., van der Wel, P. C. A., Koeppe, R. E., II, Liskamp, R. M. J., and Killian, J. A. (2004) Tilt angles of transmembrane model peptides in oriented and non-oriented lipid bilayers as determined by ^{2}H solid-state NMR. *Biophys. J. 86*, 3709−3721.

(27) Nevzorov, A. A., Mesleh, M. F., and Opella, S. J. (2004) Structure determination of aligned samples of membrane proteins by NMR spectroscopy. *Magn. Reson. Chem. 42*, 162−171.

(28) Saito, H., Ando, I., and Ramamoorthy, A. (2010) Chemical shift tensor: The heart of NMR: Insights into biological aspects of proteins. *Prog. Nucl. Magn. Reson. Spectrosc. 57*, 181−228.

(29) Bechinger, B., Resende, J. M., and Aisenbrey, C. (2011) The structural and topological analysis of membrane-associated polypep-

tides by oriented solid-state NMR spectroscopy: Established concepts and novel developments. *Biophys. Chem. 153*, 115−125.
(30) Vostrikov, V. V., Grant, C. V., Opella, S. J., and Koeppe, R. E., II (2011) On the combined analysis of ^{2}H and $^{15}N/^{1}H$ solid-state NMR data for determination of transmembrane peptide orientation and dynamics. *Biophys. J. 101*, 2939−2947.
(31) Ketchem, R. R., Lee, K. C., Huo, S., and Cross, T. A. (1996) Macromolecular structural elucidation with solid-state NMR-derived orientational constraints. *J. Biomol. NMR 8*, 1−14.
(32) Tian, C., Gao, P. F., Pinto, L. H., Lamb, R. A., and Cross, T. A. (2003) Initial structural and dynamic characterization of the M2 protein transmembrane and amphipathic helices in lipid bilayers. *Protein Sci. 12*, 2597−2605.
(33) Page, R. C., Kim, S., and Cross, T. A. (2008) Transmembrane helix uniformity examined by spectral mapping of torsion angles. *Structure 16*, 787−797.
(34) Pulay, P., Scherer, E. M., van der Wel, P. C. A., and Koeppe, R. E. (2005) Importance of tensor asymmetry for the analysis of H-2 NMR spectra from deuterated aromatic rings. *J. Am. Chem. Soc. 127*, 17488−17493.